

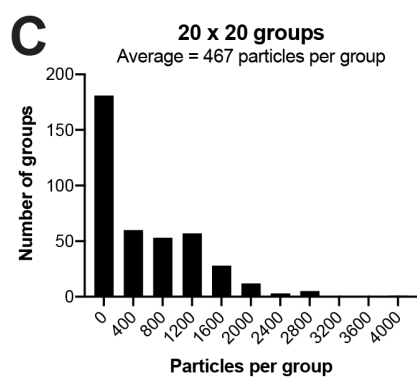
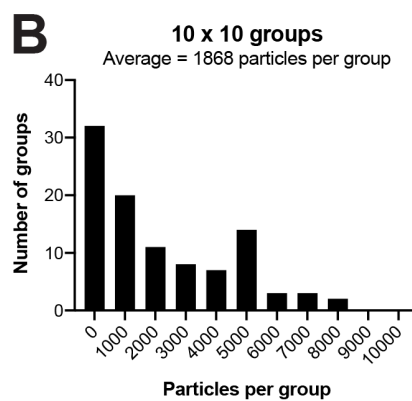
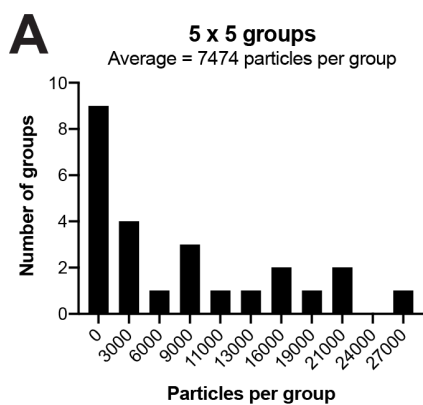
IUCrJ

Volume 8 (2021)

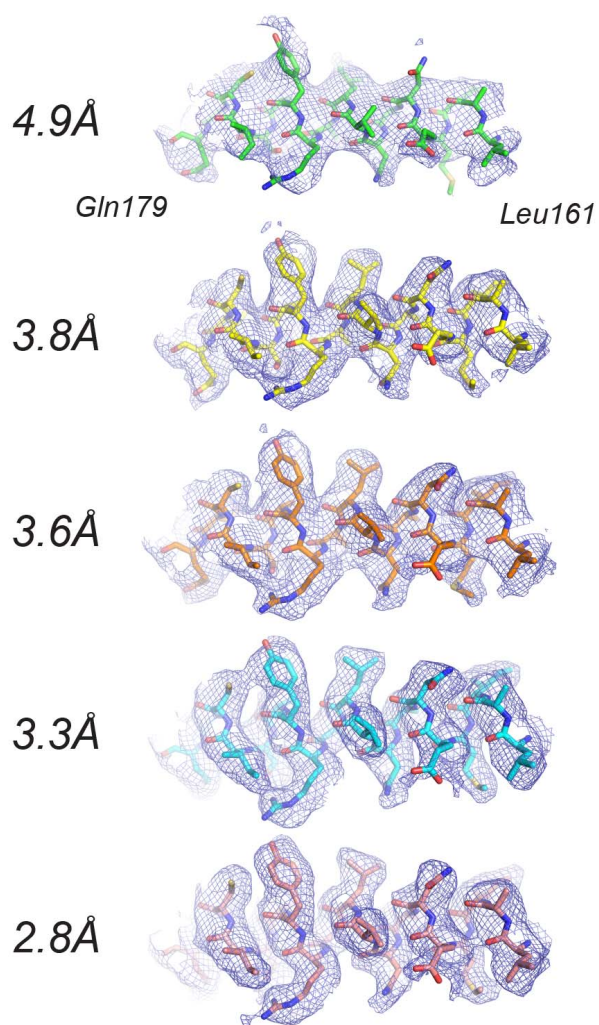
Supporting information for article:

High-resolution cryo-EM using beam-image shift at 200 keV

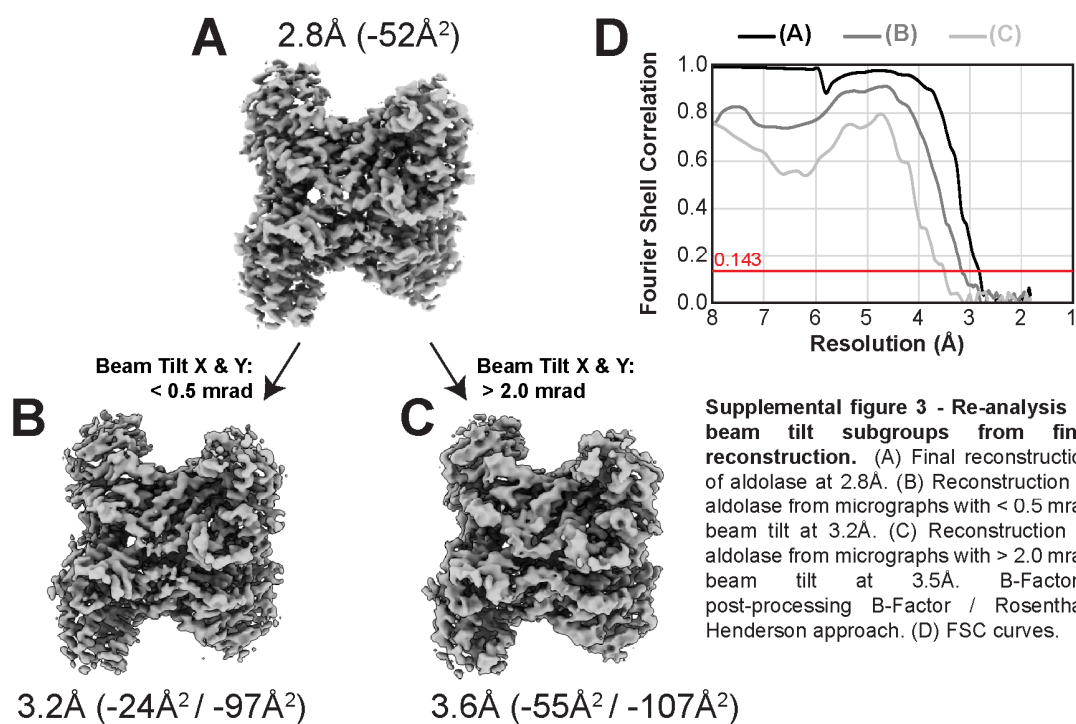
Jennifer N. Cash, Sarah Kearns, Yilai Li and Michael A. Cianfrocco

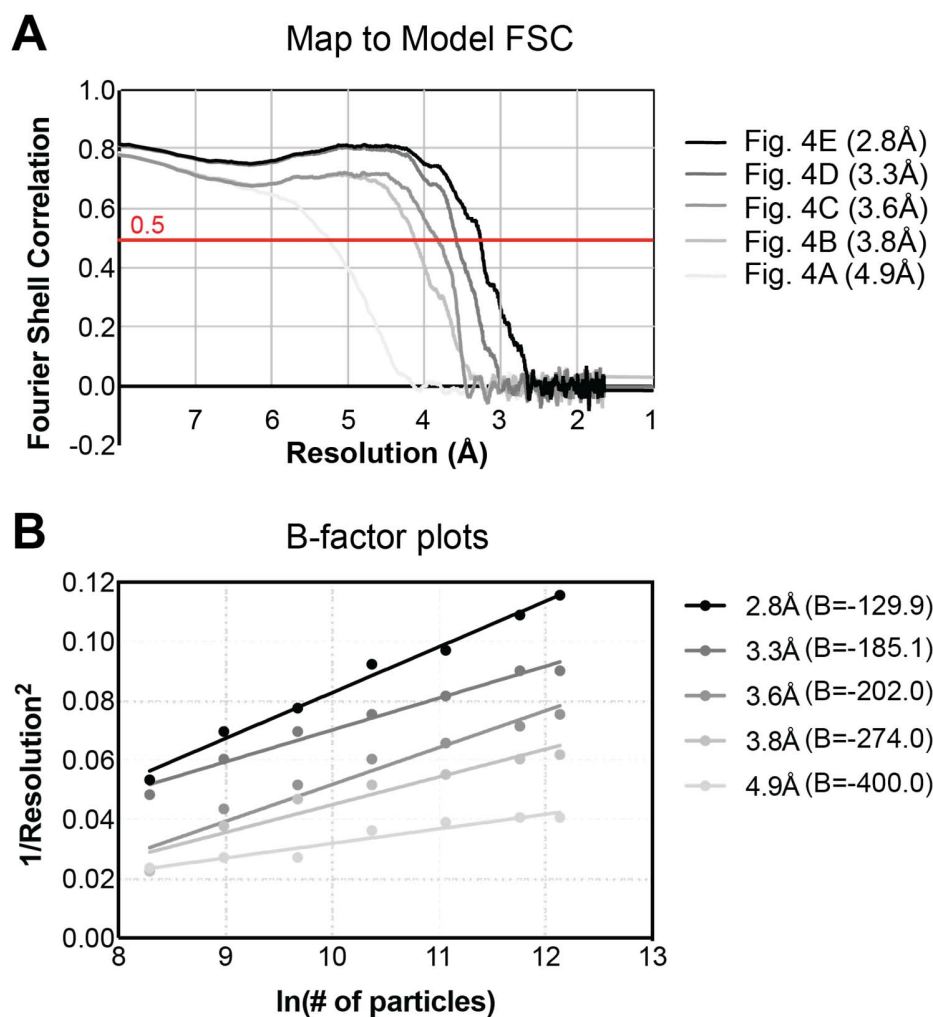


Supplemental Figure 1 - Particle numbers per group. Histograms of particle distribution per beam tilt grouping. (A) 5x5, (B) 10x10, (C) 20x20.



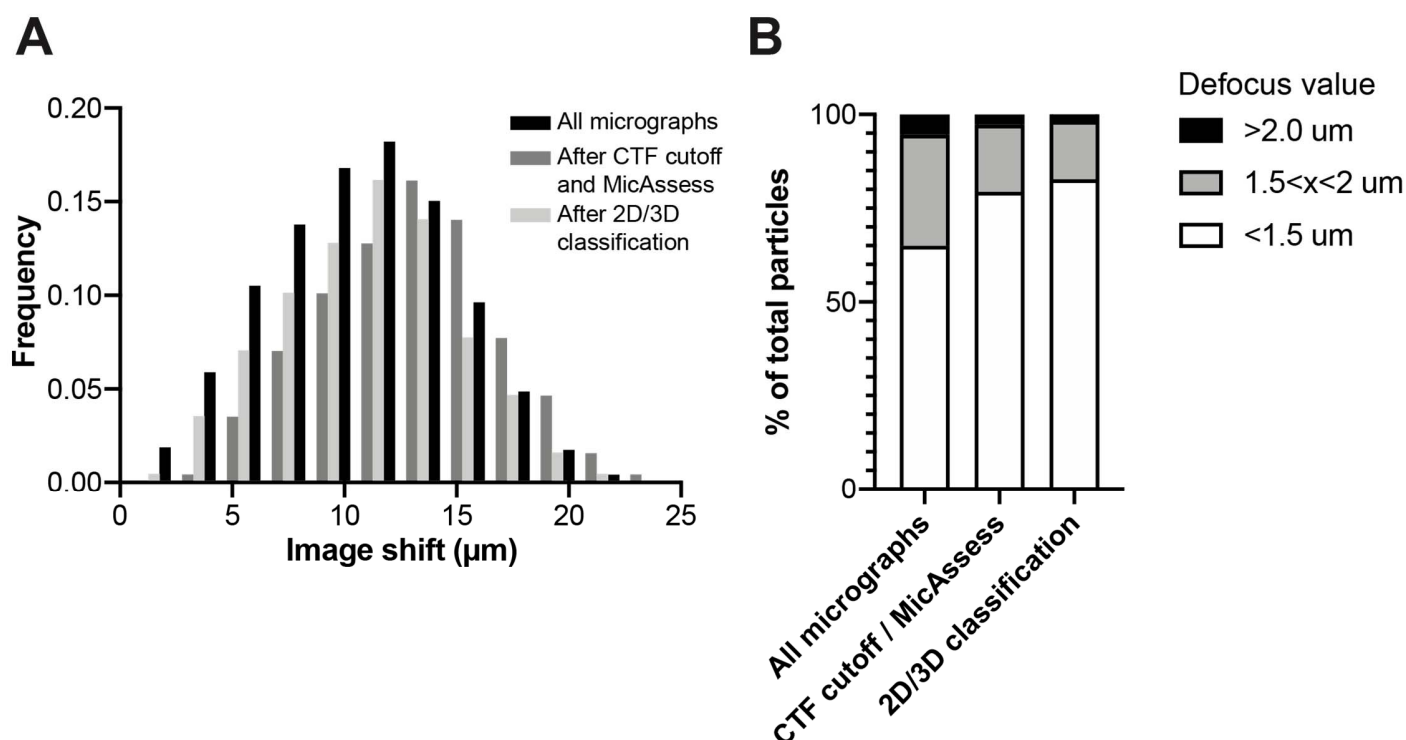
Supplemental Figure 2 - Representative densities from iterative beam-tilt refinements. Sharpened densities with associated models highlight changes in density quality through iterative rounds of beam-tilt refinement corresponding to structures from Figure 4A-4E.





Supplemental figure 4 - Structure validation during data analysis.

(A) Map-to-model FSC comparing our maps from Fig. 4A-E with 5vy5 as the model. (B) Rosenthal-Henderson plots showing particle number and resolution to determine B-factors for each reconstruction.



Supplemental figure 5 - Quantification of micrograph image shift and particle defocus. (A) For all micrographs from the dataset (black bars), the distance from (0,0) was determined and plotted as a function of frequency. The same was done for the subset of micrographs kept after CTF cut off and MicAsses (dark grey bars) and 2D/3D classification (light grey bars). (B) For every particle extracted, the defocus was binned into lower than 1.5 μm (white), higher than 2 μm (black), or inbetween (grey). The same was done for the subset if particles kept after CTFcut off and MicAsses (500,001) and 2D/3D classification (186,471 particles).

Supplemental Table S1 - Cryo-EM data collection, refinement, and validation statistics.

	Aldolase (19apr12a)
Microscope	Talos-Arctica
Detector	Gatan K2
Voltage (keV)	200
Electron exposure ($e^-/\text{\AA}^2$)	43
Defocus range (μm)	0.8 - 2
Data collection mode	Beam-image shift
Micrographs collected (per hour)	73
Original pixel size (\AA)	0.91
Symmetry imposed	D2
Initial number of micrographs	2,111
Final number of micrographs	569
Initial particle images (no.)	718,578
Final pixel size	0.91
Final particle images (no.)	186,841
Number of optics groups	400
FSC threshold	0.143
Final map resolution (\AA)	2.8
Final post-processing B-Factor (\AA^2)	-52

Supplemental Table S2 - Model building statistics.

Structure from Figure 4	4A	4B	4C	4D	4E
EMDB/PDB ID	22754/7K9L	22755/7K9X	22756/7KA2	22757/7KA3	22758/7KA4
Resolution (Å)	4.9	3.8	3.6	3.3	2.8
Postprocessing B-Factor (Å ²)	-347	-168	-105	-91	-52
B-Factor (Å²) (Rosenthal et al. 2003)	-400.0	-274.0	-202.0	-185.1	-129.9
RELION Version	3.0.2	3.0.8	3.0.8	3.1	3.1
Bonds (RMSD)					
Length (Å)	0.007	0.008	0.008	0.004	0.005
Angles (°)	1.197	0.970	0.973	0.767	0.894
Molprobit score	2.18	2.21	1.94	1.35	1.86
Clash score	9.26	6.36	6.08	3.99	4.23
Ramachandran plot (%)					
Outliers	0	0	0	0	0
Allowed	3.52	3.81	4.40	2.93	3.23
Favored	96.48	96.19	95.60	97.07	96.77
Rotamer outliers (%)	3.96	6.12	2.52	0.36	3.96
CaBLAM outliers (%)	3.54	2.95	2.95	2.95	2.65

CC (mask)	0.78	0.81	0.83	0.82	0.82
CC (box)	0.67	0.79	0.87	0.76	0.77
CC (peaks)	0.58	0.71	0.80	0.72	0.73
CC (volume)	0.79	0.81	0.83	0.81	0.81
RMSD (Å) all atoms compared to Figure 4E	1.01	0.80	0.84	0.62	-
Resolution values of map- to-model FSC from Supplemental Figure 4 (Å)	5.3	4.1	3.8	3.6	3.2